Structured light vision based pipeline tracking and 3D reconstruction method for underwater vehicle

Junfeng Fan, Yaming Ou, Xuan Li, Chao Zhou, and Zengguang Hou, *Fellow, IEEE*

***Abstract*—The inspection of underwater pipeline by underwater vehicles is of great significance to ensure safe transportation. However, most of underwater pipeline inspection methods have disadvantages such as low precision, low resolution and less information, and cannot realize the fine three-dimensional (3D) reconstruction of underwater pipelines. In order to address these problems, an underwater pipeline tracking and 3D reconstruction method for underwater vehicle based on structured light vision (SLV) is proposed. Firstly, a dual-line laser SLV is developed, and a new underwater pipeline positioning method is proposed, which can simultaneously obtain the lateral deviation, height deviation and heading deviation of underwater vehicle and underwater pipeline under weak light water environment. Then, by combining laser stripe image feature points, refracted underwater SLV model and Doppler Velocity Log (DVL) information, underwater pipeline tracking and dense 3D reconstruction are realized. Finally, by integrating the self-designed underwater SLV sensor with the underwater vehicle BlueROV, an underwater pipeline tracking and 3D reconstruction system is developed. A series of planar and spatial pipeline tracking and 3D reconstruction experiments demonstrate the effectiveness of the proposed method.**

***Index Terms*—Underwater vehicle, structured light vision, underwater pipeline, underwater 3D reconstruction.**

I. Introduction

With the rapid growth of energy demand, the development of marine oil and gas resources has achieved rapid development. As the most economical and reliable way of long-distance transportation of marine oil and gas resources, underwater pipelines have been widely used. However, underwater environment is harsh, and underwater pipelines are susceptible to long-term damage due to underwater pressure, water flow erosion, and seawater corrosion. Once underwater pipelines are damaged, they not only cause huge economic losses, but also pose a serious threat to the marine environment. Therefore, regular inspection of underwater pipelines is of great significance for ensuring safe transportation [1].

As an important tool for the development of marine resources, underwater vehicles have attracted more attention due to advantages of strong motion ability and high automation level [2]–[5]. In recent years, underwater vehicles have been used to replace divers in completing underwater pipeline inspection, improving the efficiency and automation level [6], [7]. The inspection of pipelines by underwater vehicles mainly relies on carrying sensors to realize underwater pipeline tracking and pipeline information acquisition. Common sensors for underwater pipeline inspection include acoustic sensors, magnetic sensors, and optical sensors. Acoustic sensors have the advantages of long measurement distances and are not affected by water turbidity [8]. Acoustic inspection sensors mainly consists of synthetic aperture sonar, side scan sonar, multi beam bathymeter, and multi beam forward looking sonar. Torstein et al. [9] completed underwater pipeline inspection using synthetic aperture sonar mounted on both sides of the underwater vehicle. Carballini et al. [10] also used synthetic aperture sonar to identify and track underwater pipeline. Bagnitsky et al. [11] proposed an underwater pipeline inspection method based on side scan sonar. Firstly, a filtering algorithm based on gradient model is used to obtain pipeline edge points in the image, and then the Hough transform is used to determine the pipeline position. Bharti et al. [12] proposed a method for underwater pipeline detection and tracking based on a multi beam bathymeter. This method can overcome the interference of noise data and achieve robust tracking of underwater pipelines. Kasetkasem et al. [13] used forward looking sonar images to locate and extract underwater pipeline. Firstly, a pipeline detection algorithm considering the segmented linear shape of pipelines was proposed. Then, self-organizing mapping was used to connect the marked segments together to form a pipeline trajectory for underwater vehicle navigation. However, acoustic methods have shortcomings such as low measurement accuracy and low resolution, which is not suitable for the fine inspection of underwater pipelines such as underwater pipeline three-dimensional (3D) reconstruction.

Compared with acoustic methods, magnetic sensors are suitable for detecting underwater buried pipelines. Xiang et al. [14] proposed a method for underwater pipeline positioning and tracking based on magnetic sensing. Firstly, two three-axis magnetometers were used to locate the underwater pipeline and calculate the horizontal deviation and heading deviation of the underwater pipeline. Then, the magnetic line of sight

This work was supported by the Beijing Natural Science Foundation under Grant 4232057, and in part by the National Natural Science Foundation of China under Grant 62373354, 62003341, 62203250 and 62173327, and in part by the Youth Innovation Promotion Association of CAS under Grant 2022130, and in part by the Young Elite Scientists Sponsorship Program of China Association of Science and Technology under Grant YESS20210344 and YESS20210289. (Corresponding author: Yaming Ou; Xuan Li.)

Junfeng Fan, Yaming Ou and Chao Zhou are with the Laboratory of Cognition and Decision Intelligence for Complex Systems, Institute of Automation, Chinese Academy of Sciences, Beijing 100190, China (e-mail: junfeng.fan@ia.ac.cn; ouyaming2021@ia.ac.cn; chao.zhou@ia.ac.cn). Also, Yaming Ou is with the School of Artificial Intelligence, University of Chinese Academy of Sciences, Beijing, 100049, China.

Xuan Li is with the Peng Cheng Laboratory, Shenzhen 518000, China (email: lix05@pcl.ac.cn).

Zengguang Hou is with the State Key Laboratory of Multimodal Artificial Intelligence, Institute of Automation, Chinese Academy of Sciences, Beijing 100190, China (e-mail: zengguang.hou@ia.ac.cn).

navigation method was used to achieve automatic tracking of the underwater pipeline. Bharti et al. [15] used electromagnetic sensors to measure the position of underwater pipelines on a two-dimensional plane, and then an extended Kalman filter was adopted to track underwater pipelines. Chen et al. [16] located the underwater pipeline and obtained the direction and axis position of the pipeline by measuring the external magnetic field of the pipeline. However, magnetic methods have the disadvantage of low information content and is mainly used for pipeline positioning, which is also unsuitable for the fine inspection of underwater pipelines.

Optical methods have the advantages of large measurement information, high accuracy, and low cost, which have been widely used in close inspection of underwater pipelines [17]. Underwater optical methods mainly include passive vision methods and active vision methods [18]. Passive vision methods only use ambient light or underwater lighting to illuminate the scene, and realize 3D measurement based on binocular stereo vision principle [19]. Rayhana et al. [20] proposed an underwater pipeline inspection method based on passive vision and an improved MaskRCNN was presented to realize pipeline defect detection. Narimani et al. [21] presented an underwater pipeline tracking system based on monocular passive vision. Firstly, the edge detection operator and Hough transform are used to calculate the expected heading, and then an adaptive sliding mode controller is used to complete pipeline tracking. Gian et al. [22] detected pipeline boundaries from underwater image sequences and estimated the relative position and direction between underwater vehicle and pipeline using an extended Kalman filter (EKF). Allibert et al. [23] proposed an underwater pipeline tracking method based on visual servo. This method utilizes pipeline boundary image coordinates as feedback information and considers both kinematic and dynamic models in the control system. However, due to the severe absorption and scattering of light by water, the passive light vision pipeline inspection method is difficult to apply in weak light and turbid water environments.

As a representative of active vision methods, underwater structured light vision (SLV) utilizes the high penetration of blue and green laser in water, which has the advantages of good robustness and high measurement accuracy [24]. In recent years, underwater SLV methods have also been applied in underwater pipeline inspection. Inzartsev et al. [25] proposed an underwater pipeline tracking method based on SLV. Firstly, the center profile of the laser stripe is extracted, and the shape and direction of the pipeline is determined by combining with geometric feature analysis. Then, based on the position and heading deviation between the underwater vehicle and the pipeline, the tracking of the underwater pipeline is completed. However, the effectiveness of this method has only been verified by simulation experiments, and no actual experiment system is set up. Moreover, the direction of the pipeline is determined with single laser SLV sensor resulting in significant errors. Gunatilake et al. [26] proposed a pipeline internal inspection system, which is mainly composed of a mobile vehicle and a SLV sensor. This system has been applied in underground pipeline and achieve 3D reconstruction of the interior of the pipeline. Montoya et al. [27] developed a pipeline inspection system composed of an underwater vehicle and a SLV sensor, which also realized dense 3D reconstruction of the interior of the pipeline. For underwater pipelines, it is also very important to use underwater vehicles for external inspection, because some information of underwater pipelines, such as the external morphology and location of underwater pipelines, can only be obtained through external inspection. In addition, the external inspection of the pipeline is more challenging than the internal inspection of the pipeline, because the underwater vehicle needs to track the pipeline. However, the existing methods of external inspection of underwater pipelines have the disadvantages of low precision, low resolution and less information, and cannot realize the dense 3D reconstruction of the exterior of underwater pipelines.

In order to solve the above problems, we propose an underwater pipeline tracking and 3D reconstruction method for underwater vehicle based on SLV. To the best of our knowledge, this is the first underwater vehicle system that can simultaneously achieve underwater pipe tracking and dense reconstruction. The innovations of this paper are as follows:

1) A novel underwater pipeline positioning method based on dual-line laser SLV is proposed, which can simultaneously obtain the lateral deviation, height deviation and heading deviation of underwater vehicle and underwater pipeline under weak light water environment, providing the basis for underwater pipeline tracking.
2) By combining laser stripe image feature points, refracted underwater SLV model and Doppler Velocity Log (DVL) information, the tracking and dense 3D reconstruction of underwater pipeline are realized, which is difficult for existing underwater inspection methods.
3) By integrating the self-designed underwater SLV sensor with the underwater vehicle BlueROV, an underwater pipeline tracking and 3D reconstruction system is developed, and a series of planar and spatial pipeline experiments are carried out to verify its effectiveness.

II. System description

In this section, an overview of proposed underwater pipeline tracking and 3D reconstruction system is introduced, including system design and underwater SLV sensor design.

A. System design

As shown in Fig. 1, the experiment system mainly includes an underwater SLV sensor, an industrial computer, a DVL, and an underwater vehicle. Underwater SLV is used to collect laser stripe images and transmit the collected images to industrial computer through Ethernet realizing 3D point cloud computing. The industrial computer is Intel NUC11TNHi7, which communicates with DVL through a serial port. DVL is a waterlinked A50 that can provide underwater vehicle speed information of approximately 12Hz, with a maximum measurement height of 50m to the bottom. The underwater vehicle is BlueROV that is connected to an industrial computer through a fathom-X interface board. The industrial computer could obtain pipeline tracking deviation, and send it to the

Fig. 1. Schematic diagram of experimental system.

TABLE I
HARDWARE PARAMETERS OF THE DEVELOPED SYSTEM

Component	Parameters	Value
Camera	Resolution	1280×1024 pixels
	Frames	90Fps
	Focal length	12mm
Laser	Wavelength	450nm
	Power consumption	160mw
	Pattern	Two parallel stripes
SLV	Dimensions	126×100×52mm
	Weight	0.8Kg
DVL	Frequency	12Hz
	Measurement distance	50m

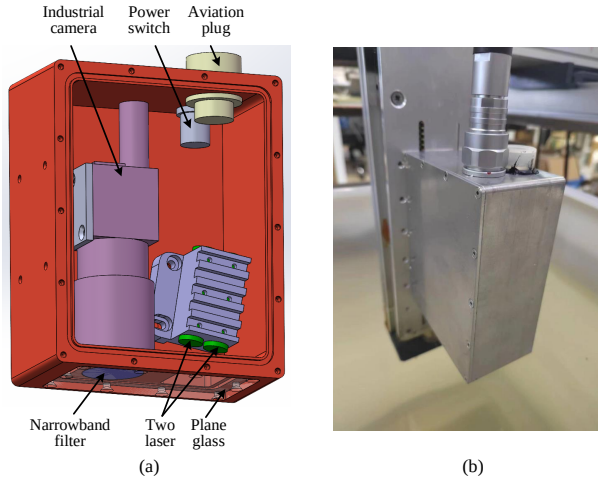

Fig. 2. The design of the SLV sensor. (a) The 3D model. (b) The physical device.

BlueROV. The controllers in the BlueROV including Raspberry Pi 3B+ and STM32F407 are used to complete the motion control. The hardware parameters of the experimental system components are shown in Table I.

B. Underwater SLV sensor design

As shown in Fig. 2, underwater SLV sensor mainly consists of an industrial camera, two lasers, a narrowband filter, a transparent glass and a waterproof shell. The industrial camera is MER2-134-90. Its frame rate is 90Fps and resolution is 1280×1024. To determine the direction of the underwater

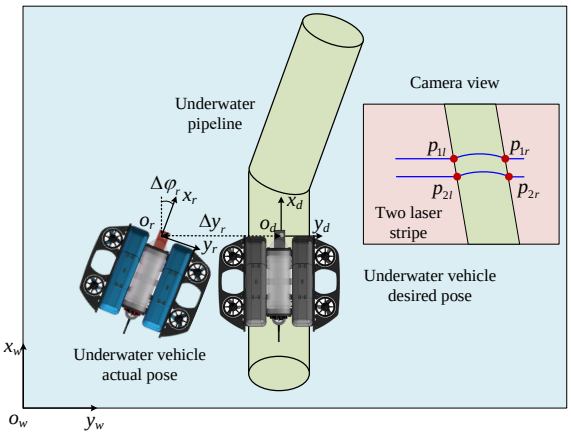

Fig. 3. Schematic diagram of underwater pipeline tracking.

pipeline, two lasers are adopted, which can project two parallel laser stripes onto the underwater pipeline. Because of the small attenuation of blue-green light in water, the wavelength of laser is 450nm and laser power is 80mw. To eliminate the influence of backscattering in water on acquired images, a narrowband filter is installed in front of the lens, and its central wavelength is also set as 450nm. The camera and laser are installed in a waterproof shell, and the relative installation angle of them can be adjusted based on the working distance. The transparent glass is installed in front of the camera and laser, and its thickness is 3mm.

III. UNDERWATER PIPELINE TRACKING

A. Problem description and algorithm framework

The objective of this paper is to design a control algorithm that enables the underwater vehicle to track the desired underwater pipeline based on underwater SLV information. The schematic diagram of underwater pipeline tracking is shown in Fig. 3. In this paper, $o_w x_w y_w z_w$ is the world coordinate system, and $o_r x_r y_r z_r$ and $o_d x_d y_d z_d$ are the accompanying coordinate system of the actual and expected pose of the underwater vehicle, respectively. The forward velocity of the underwater vehicle is v_x, the lateral velocity is v_y, the vertical velocity is v_z, and the yaw angular velocity is w. The lateral position deviation of underwater vehicle can be expressed as $\Delta y = f_1(laser1, laser2)$, the vertical position deviation of underwater vehicle can be expressed as $\Delta z = f_2(laser1, laser2)$, and the heading angle deviation of underwater vehicle can be expressed as $\Delta\varphi = f_3(laser1, laser2)$. The control objectives of underwater pipeline tracking can be expressed as:

$$\begin{cases} \lim\limits_{t\to\infty} \Delta y = 0 \\ \lim\limits_{t\to\infty} \Delta z = 0 \\ \lim\limits_{t\to\infty} \Delta\varphi = 0 \end{cases} \tag{1}$$

According to the above description, the algorithm framework of this paper mainly includes underwater pipeline positioning and underwater pipeline tracking control. Among

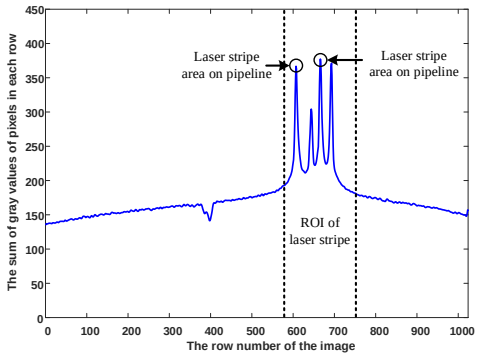

(a)

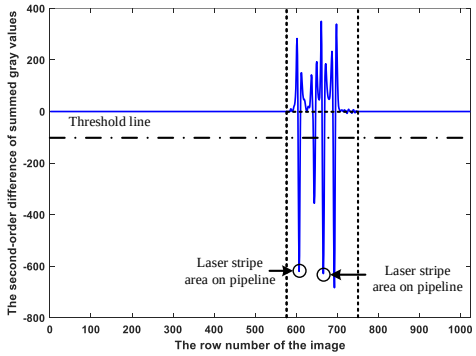

(b)

Fig. 4. The determination of laser stripe regions on the pipeline (a) Sum result of gray values in each row. (b) The second-order difference of summed gray values

them, underwater pipeline positioning is to obtain underwater pipeline information and calculate the underwater vehicle motion deviation $\Delta y, \Delta z, \Delta\varphi$ based on underwater SLV sensor. Underwater pipeline tracking control is to calculate the control output v_y, v_z, w based on three motion deviations.

B. Underwater pipeline positioning

In this paper, underwater pipeline positioning is realized by using the developed underwater SLV sensor. Firstly, the laser SLV image is processed to extract the region of interest (ROI) of the laser stripe. Due to the fact that the laser stripes are approximately parallel to the u-axis of the image and the pixel grayscale values in the laser stripe area are relatively high, the gray values of each row of pixels are summed. The sum result of the pixel gray values along the u-axis is shown in Fig. 4(a).

The image size of laser SLV image is 1280×1024, and the ROI of laser stripes can be determined as follows:

$$\begin{cases} [x_{lmin}, x_{lmax}] = [1, 1280] \\ [y_{lmin}, y_{lmax}] = [v_l - h_l, v_l + h_l] \end{cases} \tag{2}$$

Where v_l is the row index with the maximum sum result, and h_l is the width of the laser stripe ROI.

In the above ROI of laser stripe, the region of the laser stripe located on the pipeline need to be determined. It can be seen from Fig. 4(a) that there are four local maximum points in the ROI of laser stripe, among which the regions near the first and third local maximum points are the laser stripe regions on the

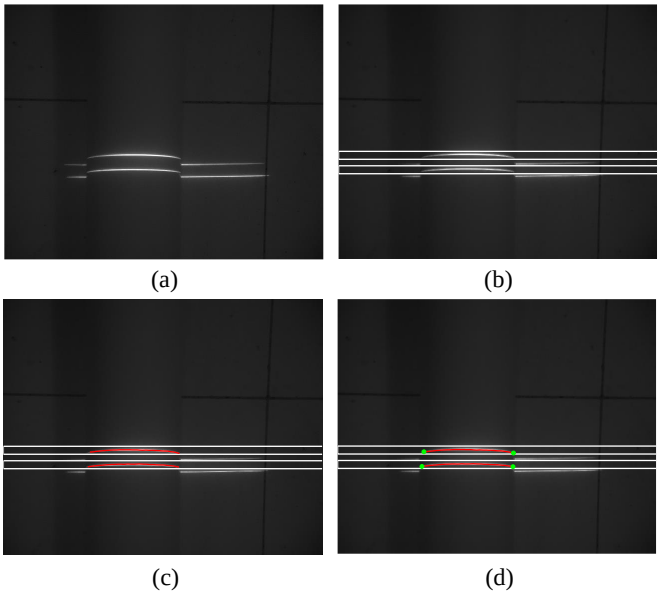

(a) (b) (c) (d)

Fig. 5. Image processing process. (a) Original image (b) Laser stripe area on the pipeline. (c) Center profile of laser stripe. (d) Feature points.

pipeline. Then, a second-order difference operator is designed to locate laser stripe regions on the pipeline.

$$T(i) = \sum_{k=-n}^{n} s(i+k) - (2n+1)\, s(i) \tag{3}$$

The second-order difference of summed gray values is shown in Fig. 4(b). By setting a threshold, the laser stripe regions on the pipeline can be obtained with Eq. (4).

$$\begin{cases} [y_{l1min}, y_{l1max}] = [v_{l1} - h_t, v_{l1} + h_t] \\ [y_{l2min}, y_{l2max}] = [v_{l2} - h_t, v_{l2} + h_t] \end{cases} \tag{4}$$

Where v_{l1} and v_{l2} are the first and third local minimum points during the second-order difference of summed gray values, and h_t is the width of the laser stripe region on the pipeline.

Then, in the laser stripe area on the pipeline, the Ostu method is adopted to realize adaptive threshold segmentation, and the connected domain area is counted to remove noise points. Finally, the widely used gray gravity center method is adopted to obtain the center profile points of the laser stripe.

The above image processing method has been verified on several underwater pipeline images. The complete image processing process is shown in Fig. 5. The results show that the method can accurately detect feature points of underwater pipeline.

After obtaining the image coordinates of the left and right boundary feature points of two laser stripes, their 3D coordinates in the camera coordinate system can be obtained based on the underwater SLV measurement model. Then, the pose information of the underwater pipeline feature points in the vehicle coordinate system can be expressed with Eq. (5).

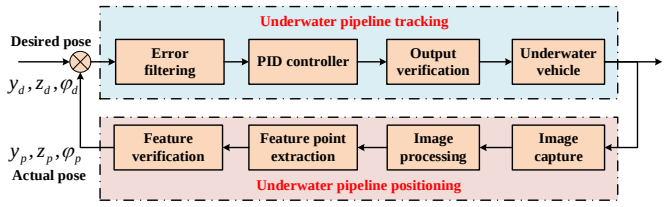

Fig. 6. Schematic diagram of underwater pipeline tracking control.

$$\begin{cases} x_p = \left(x_{p1l} + x_{p1r} + x_{p2l} + x_{p2r}\right)/4 \\ y_p = \left(y_{p1l} + y_{p1r} + y_{p2l} + y_{p2r}\right)/4 \\ z_p = \left(z_{p1l} + z_{p1r} + z_{p2l} + z_{p2r}\right)/4 \\ \varphi_p = \tan^{-1}\frac{\left(y_{p1l}+y_{p1r}-y_{p2l}-y_{p2r}\right)}{\left(x_{p1l}+x_{p1r}-x_{p2l}-x_{p2r}\right)} \end{cases} \tag{5}$$

Finally, underwater vehicle motion deviation can be determined with Eq. (6).

$$\begin{cases} \Delta y = y_d - y_p \\ \Delta z = z_d - z_p \\ \Delta \varphi = \varphi_d - \varphi_p \end{cases} \tag{6}$$

Where y_d and φ_d are set as 0.

C. Underwater pipeline tracking control

1) Feature verification: Due to the complex underwater environment, some feature points may not be accurately extracted during the underwater pipeline tracking process. If incorrect feature points are directly used as feedback, it will immediately increase the deviation between the underwater vehicle and the underwater pipeline, leading to the failure of underwater pipeline tracking. Therefore, feedback feature verification is required. According to the slow change of feature points in adjacent sampling periods, feedback feature verification can be expressed with Eq. (7).

$$\begin{cases} |u_p(t) - u_p(t-1)| < u_T \\ |v_p(t) - v_p(t-1)| < v_T \end{cases} \tag{7}$$

The image coordinates of underwater pipeline feature points are:

$$\begin{cases} u_p = \left(u_{p1l} + u_{p1r} + u_{p2l} + u_{p2r}\right)/4 \\ v_p = \left(v_{p1l} + v_{p1r} + v_{p2l} + v_{p2r}\right)/4 \end{cases} \tag{8}$$

Where u_T and v_T are the two thresholds. If the feedback characteristics satisfy Eq. (7), it could be used in the controller. Otherwise it will be considered a false feature.

2) Tracking controller: When the feedback feature satisfies Eq. (7), it is saved to the data queue. However, there exist errors in the obtained image features. Gaussian filtering method is used to reduce the influence of these measurement errors.

$$e_j = \frac{\sum_{i=1}^{n} \alpha_i e(i)}{\sum_{i=1}^{n} \alpha_i} \tag{9}$$

Where e_j is the filtering error of the j-th control cycle, α_i is the filter coefficient.

Due to the simplicity and reliability of the Proportional-Integral- Differential (PID) controller, PID controller is adopted to achieve lateral position control, vertical position control, and heading control of underwater vehicle.

$$u_k = K_p e_k + K_i \sum_{j=0}^{k} e_j + K_d \left(e_k - e_{k-1}\right) \tag{10}$$

Where u_k is the output of the sampling period k, and k_p, k_i and k_d are the three parameters of the PID controller.

The control quantity u_k is the speed control quantity of the underwater vehicle. Based on the secondary development program Ardusub, u_k is send to underwater vehicle controller to realize underwater pipeline tracking.

During underwater pipeline tracking process, stability is an important factor to ensure the quality of underwater pipeline 3D reconstruction. In order to ensure the stability of underwater robot motion, under the premise of ensuring that the pipeline is within the field of view, underwater pipeline tracking should be smooth. Therefore, the output of each control cycle should be less than a threshold. Meanwhile, due to the significant impact of heading adjustment on the actual lateral position, pipelines are prone to loss in the field of view when both heading and lateral positions are adjusted simultaneously. Therefore, when the heading deviation is less than a certain threshold, the heading is not adjusted, only the lateral and vertical positions are adjusted. When the heading deviation exceeds the set threshold, the heading is adjusted firstly, and the lateral position is not adjusted at this time.

IV. Underwater Pipeline 3D Reconstruction

A. Basic principle

The basic principle of underwater pipeline 3D reconstruction is shown in Fig. 7. During the process of underwater pipeline tracking, underwater SLV sensor captures the underwater pipeline image in real time and obtains the image coordinates of the center profile points of the laser stripe. Then, combined with the underwater SLV measurement model, the 3D coordinates of the center profile points of the laser stripe in the camera coordinate system are obtained. Besides, the 3D coordinates of the center profile points of the laser stripe in the vehicle coordinate system are obtained by combining the transformation matrix of camera and DVL. Finally, by fusing the dead reckoning results of the underwater vehicle, the 3D coordinates of the center profile points of the laser stripe in the world coordinate system are obtained, so as to complete the 3D reconstruction of the underwater pipeline.

B. Underwater SLV measurement model

The underwater SLV measurement model is shown in Fig. 8, which considers the refraction influence on the camera imaging model and the laser plane model. The camera coordinate system is $oxyz$ and the origin o is the camera optical center. Its z axis is the camera optical axis, and the x axis and y axis are parallel with the horizontal and vertical coordinates of the

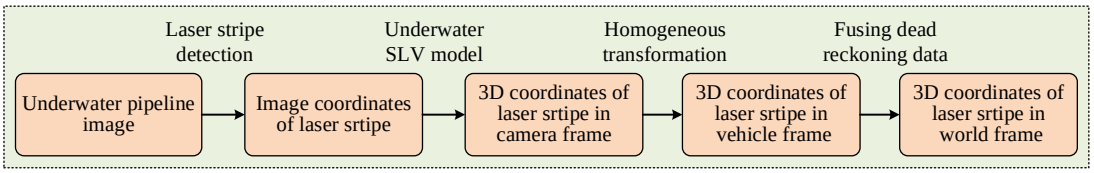

Fig. 7. Schematic diagram of underwater pipeline 3D reconstruction.

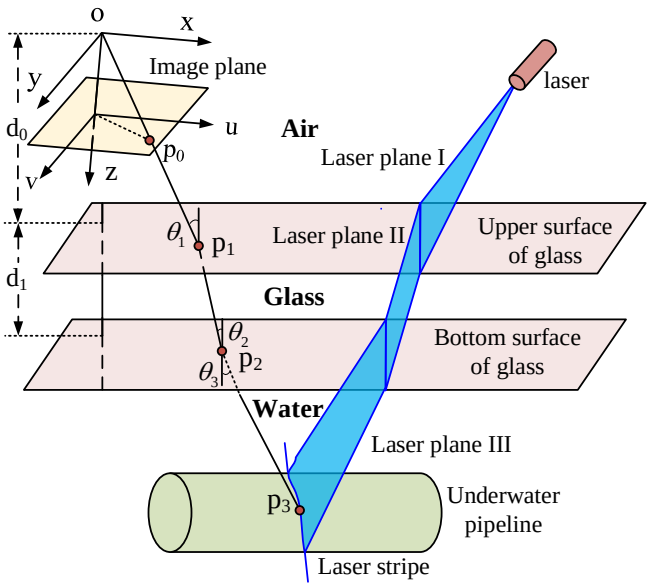

Fig. 8. Underwater SLV measurement model.

image plane respectively. Define the feature point of the laser stripe on the image plane is p_0, the intersection point of the ray op_0 and the upper surface of the glass is p_1, the refraction ray of op_0 through the upper surface of the glass is p_1p_2, and the refraction ray of p_1p_2 through the lower surface of the glass is p_2p_3. The included angles of ray op_1, p_1p_2 and p_2p_3 and normal vector of glass surface are θ_1, θ_2 and θ_3, respectively.

Assuming that the equation of laser plane I is $A_1x+B_1y+C_1z+D_1=0$, it can be obtained using calibration method in [28]. Assuming that the unit normal vector $\boldsymbol{n}$ of the glass surface is (a,b,c), and the distance from the camera optical center to the upper surface of the glass is d_0, which can be determined with calibration method in [29]. Then, the plane equation of the upper surface of the glass is $ax+by+cz-d_0=0$. Assume that the plane equation of laser plane II is $A_2x+B_2y+C_2z+D_2=0$. Then the parameters of laser plane II can be obtained with Eq. (11).

$$\begin{cases} A_2 = \frac{-(\lambda_1\gamma_1+\alpha_1\beta_1)\pm\sqrt{(\lambda_1\gamma_1+\alpha_1\beta_1)^2-(1+{\gamma_1}^2+{\beta_1}^2)({\alpha_1}^2+{\lambda_1}^2-1)}}{(1+{\gamma_1}^2+{\beta_1}^2)} \\ B_2 = \lambda_1+\gamma_1A_2 \\ C_2 = \alpha_1+\beta_1A_2 \\ D_2 = C_2\left(D_1-k_1d_0\right)/\left(C_1+k_1c\right) \end{cases} \tag{11}$$

The parameters of λ_1, γ_1, α_1, β_1, and k_1 can be determined with Eq. (12).

$$\begin{cases} \lambda_1 = \frac{u_{air}(aA_1+bB_1+cC_1)(acB_1-bcA_1)}{u_{glass}[b(acB_1-bcA_1)-c(c^2A_1-acC_1)]} \\ \gamma_1 = \frac{c\left(bcC_1-c^2B_1\right)-a(acB_1-bcA_1)}{b(acB_1-bcA_1)-c(c^2A_1-acC_1)} \\ \alpha_1 = \frac{u_{air}(aA_1+bB_1+cC_1)\left(acC_1-c^2A_1\right)}{u_{glass}[b(acB_1-bcA_1)-c(c^2A_1-acC_1)]} \\ \beta_1 = \frac{a\left(c^2A_1-acC_1\right)-b\left(bcC_1-c^2B_1\right)}{b(acB_1-bcA_1)-c(c^2A_1-acC_1)} \\ k_1 = \frac{B_1C_2-B_2C_1}{cB_2-bC_2} \end{cases} \tag{12}$$

Assume that the plane equation of laser plane III is $A_3x+B_3y+C_3z+D_3=0$. Similarly, the parameters of laser plane III in water can be obtained with Eq. (13).

$$\begin{cases} A_3 = \frac{-(\lambda_2\gamma_2+\alpha_2\beta_2)\pm\sqrt{(\lambda_2\gamma_2+\alpha_2\beta_2)^2-(1+{\gamma_2}^2+{\beta_2}^2)({\alpha_2}^2+{\lambda_2}^2-1)}}{(1+{\gamma_2}^2+{\beta_2}^2)} \\ B_3 = \lambda_2+\gamma_2A_3 \\ C_3 = \alpha_2+\beta_2A_3 \\ D_3 = C_3\left(D_2-k_2\left(d_0{+}d_1\right)\right)/\left(C_2+k_2c\right) \end{cases} \tag{13}$$

Assuming the image coordinate of the point p_0 is (u,v), based on the pinhole imaging model, the direction vector $\boldsymbol{r_1}$ of op_1 can be calculated with $\left(\left(u-u_0\right)/f_x,\left(v-v_0\right)/f_y,1\right)$, where f_x, f_y, u_0 and v_0 are the intrinsic parameters of camera. Then, the 3D coordinates of p_1 in the camera coordinate system is $X_1=d_0\boldsymbol{r_1}/(\boldsymbol{r_1}\cdot\boldsymbol{n})$.

Since all rays passing through the refraction surface and the normal vector of the refraction surface are in same plane [30], there are:

$$\boldsymbol{r_{i+1}}=\rho_i\boldsymbol{r_i}+\varphi_i\boldsymbol{n_i}(i=1,2) \tag{14}$$

$$\begin{cases} \rho_i = u_i/u_{i+1} \\ \varphi_i = \sqrt{1-\left(\frac{u_i}{u_{i+1}}\right)^2\left(1-(\boldsymbol{r_i}\cdot\boldsymbol{n})^2\right)}-\frac{u_i}{u_{i+1}}\boldsymbol{r_i}\cdot\boldsymbol{n} \end{cases} \tag{15}$$

Then, the 3D coordinates of point p_2 in the camera coordinate system are:

$$X_2=X_1+\frac{d_1}{\boldsymbol{r_2}\cdot\boldsymbol{n}}\boldsymbol{r_2} \tag{16}$$

Combining with the 3D coordinates of p_2 in the camera coordinate system and the unit vector $\boldsymbol{r_3}$ expressed with

(l_3, m_3, n_3), the 3D coordinates of the p_3 in the camera coordinate system can be determined by computing the intersecting point of the refraction ray p_2p_3 and the laser plane III.

$$\begin{cases} x = -l_3 \frac{A_3x_2+B_3y_2+C_3z_2+D_3}{A_3l_3+B_3m_3+C_3n_3} + x_2 \\ y = -m_3 \frac{A_3x_2+B_3y_2+C_3z_2+D_3}{A_3l_3+B_3m_3+C_3n_3} + y_2 \\ z = -n_3 \frac{A_3x_2+B_3y_2+C_3z_2+D_3}{A_3l_3+B_3m_3+C_3n_3} + z_2 \end{cases} \tag{17}$$

C. 3D reconstruction fusing dead reckoning

In this paper, the fusion results of DVL and IMU are adopted to realize the dead reckoning of underwater vehicle. By utilizing the acoustic Doppler effect, DVL can achieve stable velocity measurement of underwater vehicle, including v_x, v_y, and v_z, typically around 12Hz. In addition, the DVL integrates Yost Labs TSS-NANO IMU, which can provide high-frequency linear acceleration and angular velocity information for underwater vehicle, with an output frequency of about 200Hz.

By fusing DVL and IMU, the dead reckoning result of underwater vehicle can be obtained, with an output frequency of about 5Hz. The dead reckoning accuracy is about $1\%D$, which is defined as the ratio of dead reckoning error to traveling distance. The point cloud output frequency of the underwater SLV sensor is about 20Hz. Therefore, the position and attitude measurement values are interpolated based on the timestamp of each image. Due to the absence of sudden acceleration caused by the large mass of the vehicle and the inertia of the surrounding water, the inaccuracy introduced by interpolation can be ignored [31]. Therefore, the transformation matrix between the vehicle coordinate system and the world coordinate system at each time can be obtained.

V. Experiments and Results

To test the performance of the proposed underwater pipeline tracking and 3D reconstruction method, a experiment scenario is established firstly. Then, the underwater SLV sensor is mounted on a three-axis moving platform to complete 3D reconstruction of regular and irregular objects to independently verify the 3D reconstruction capability. Besides, a series of planar and spatial pipeline tracking and 3D reconstruction experiments are carried out. Finally, the comparison of the state-of-art underwater pipeline inspection methods and our proposed method is discussed.

A. Experiment environment

To verify the effectiveness of the proposed system, we conducted a series of underwater pipeline tracking and 3D reconstruction experiments in a pool, and its size is about $5m \times 4m \times 1.5m$ pool. The experimental scenario is shown in Fig. 9. Notably, a global camera above pool is used to record the whole experiment process and does not participate in the control of the underwater vehicle.

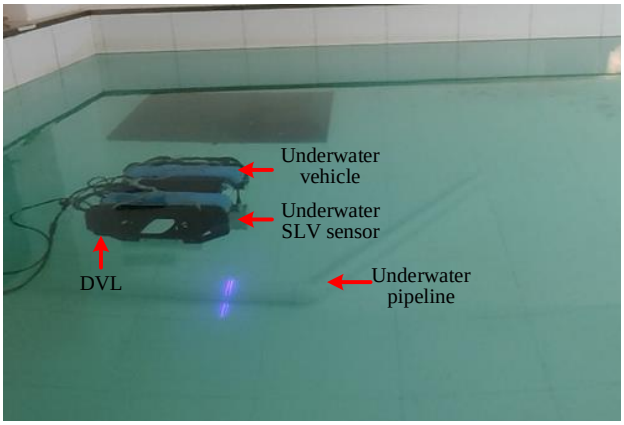

Fig. 9. Underwater pipeline tracking and 3D reconstruction experiment scene.

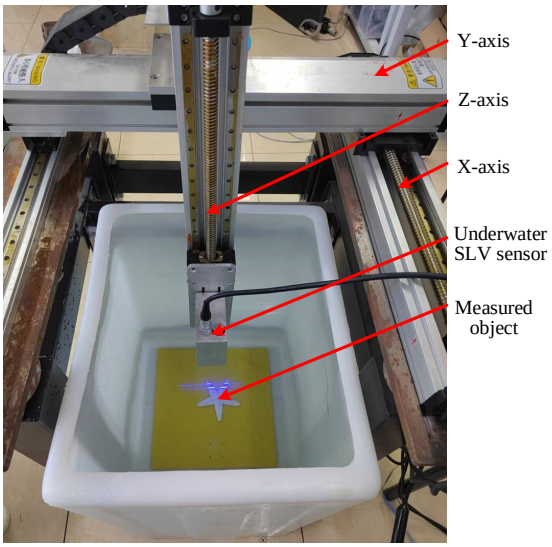

Fig. 10. Underwater stable 3D reconstruction experiment scene.

B. Underwater stable 3D reconstruction experiment

In order to independently test the 3D reconstruction performance of the developed underwater SLV sensor, we first installed it on a three-axis moving platform for scanning measurement of underwater objects, as shown in Fig. 10. In this way, the 3D reconstruction performance is mainly related with underwater SLV sensor. The X-, Y-, and Z-axes of the motion platform are driven by three stepper motors, and the SLV sensor is installed at the end of the Z-axis of the motion platform. A square object and a starfish object are placed in a tank, and the measurement distance is about 70cm. The material of the square object is aluminum alloy, and its size is 70×70mm, and the material of the starfish target is plastic. The square object and starfish object are shown in Fig. 11(a) and (b).

For square object, quantitative analysis of 3D reconstruction accuracy is conducted using plane fitting error and length measurement error. Firstly, the 3D point cloud is used for spatial plane fitting, and then the root mean square error (RMSE) of the distance between all 3D points and the fitting plane is calculated to obtain the plane fitting error. For length

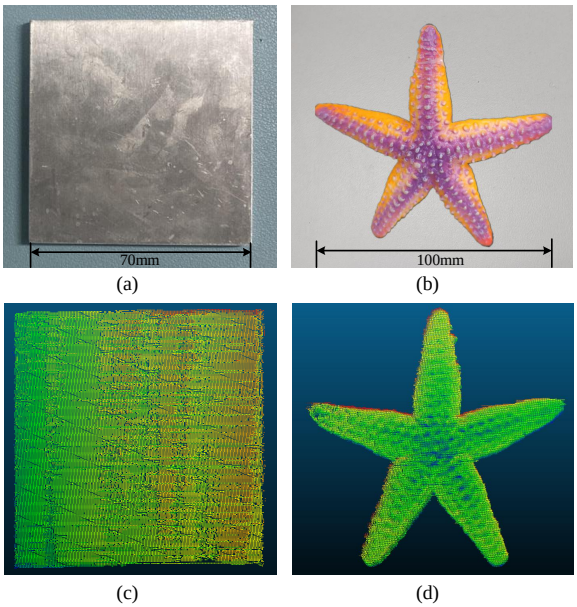

Fig. 11. Underwater stable 3D reconstruction results of different objects. (a) Square object. (b) Starfish object. (c) Reconstruction result of square object. (d) Reconstruction result of starfish object.

TABLE II
3D RECONSTRUCTION ACCURACY OF DIFFERENT OBJECTS

Object	Plane fitting error	Length error	RMSE	Average error
Square object	1.1mm	2.8mm	-	-
Starfish object	-	-	1.0mm	1.8mm

error, the average length measurement value is obtained by measuring the distance between opposite edges multiple times, and then the deviation between the measured value and the actual value is calculated to obtain the length measurement error. For starfish object, due to its irregular shape, an iterative nearest point (ICP) matching algorithm is used to quantitatively analyze the reconstruction accuracy. Firstly, a commercial depth camera (Mech Eye Nano) is used to obtain a 3D point cloud of starfish in the air as ground truth. Then, ICP matching algorithm is used to register with the point cloud obtained by the SLV sensor in water. Finally, RMSE and average error are used to represent the 3D reconstruction accuracy of starfish object. The 3D reconstruction results of square object and starfish object are shown in Fig. 11(c) and (d), and the 3D reconstruction accuracy is shown in Table II. It can be seen that the proposed underwater SLV could achieve accurate 3D reconstruction accuracy in water.

C. Planar pipeline tracking and 3D reconstruction experiments

Planar straight pipeline and curved pipeline tracking and 3D reconstruction experiments are carried out to verify the performance of the proposed method.

1) Straight pipeline: The total length of the underwater straight pipeline is about 1.4m, and the diameter of the pipeline is 7.5cm, which is arranged at the bottom of the pool. The underwater vehicle with the developed underwater SLV sensor

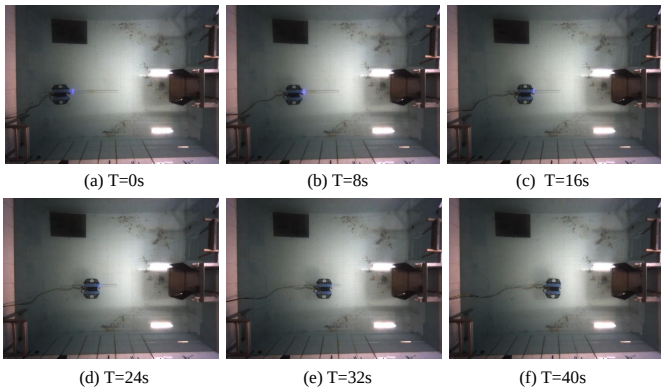

Fig. 12. Image sequences of the underwater straight pipeline tracking.

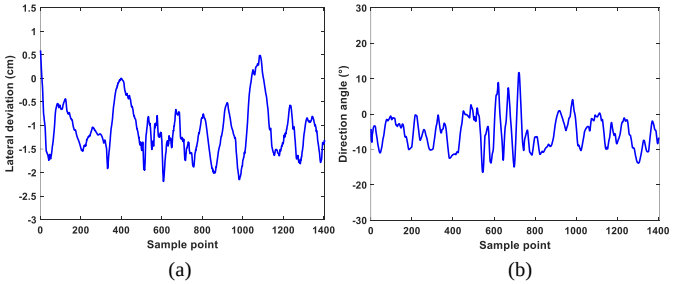

Fig. 13. Underwater straight pipeline tracking. (a) Lateral position deviation. (b) Direction angle.

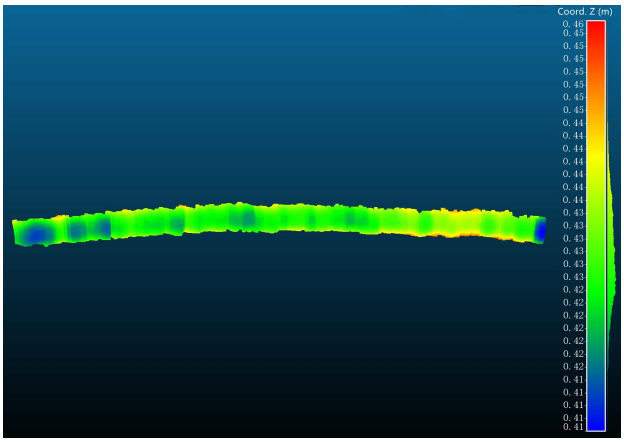

Fig. 14. 3D reconstruction result of underwater straight pipeline.

is used to realize pipeline tracking and 3D reconstruction, and the working distance of the underwater SLV sensor is about 45cm. The video capture sequence of the underwater straight pipeline tracking experiment is shown in Fig. 12. It can be seen that the proposed system can track the underwater straight pipeline well.

In order to conduct quantitative analysis of pipeline tracking performance, we analyzed the lateral position deviation and direction angle in the process of underwater pipeline tracking, which can be obtained with Eq. (6). As shown in Fig. 13, the lateral position deviation of the underwater vehicle is within 2.5cm, and its average deviation is 1.1cm. The average direction angle is 5.8°. In addition, the 3D reconstruction result

TABLE III
PLANAR PIPELINE TRACKING AND 3D RECONSTRUCTION PERFORMANCE

Object	Lateral deviation	Direction angle	Diameter error
Straight pipeline	2.5cm	5.8°	5.7mm
Curved pipeline	3.0cm	5.3°	4.5mm

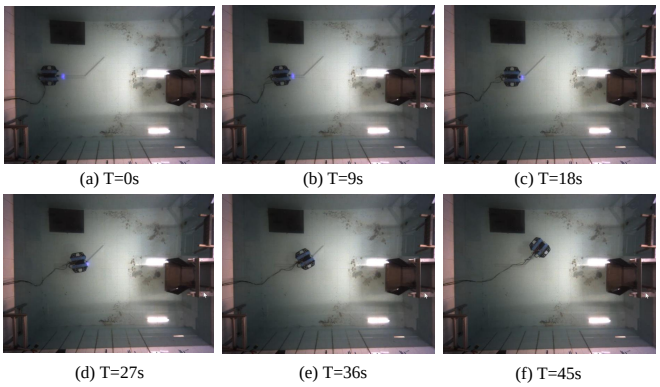

(a) T=0s (b) T=9s (c) T=18s (d) T=27s (e) T=36s (f) T=45s

Fig. 15. Image sequences of the underwater curved pipeline tracking.

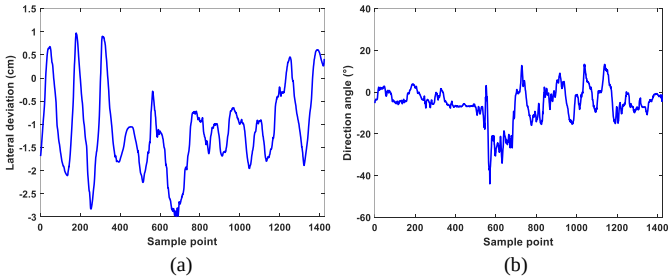

(a) (b)

Fig. 16. Underwater curved pipeline tracking. (a) Lateral position deviation. (b) Direction angle.

of the underwater straight pipeline is shown in Fig. 14. It can be seen that the basic shape of the acquired point cloud is consistent with the actual pipeline. We measured the diameter of the pipeline at different locations in the point clouds, and the average measurement error of the pipeline diameter was 5.7mm. The above experimental results show that the proposed SLV based underwater pipeline tracking and 3D reconstruction method could get satisfactory performance.

2) Curved pipeline: To verify the robustness of the proposed method, we conducted underwater curved pipeline tracking and 3D reconstruction experiments. The curved pipeline consists of a straight pipeline 1 with a length of 0.6m, a 45° turning joint, and a straight pipeline 2 with a length of 0.8m. The video collection sequence of the underwater curved pipeline tracking experiment is shown in Fig. 15. It can be seen that the proposed system could also track underwater curved pipeline.

In order to quantitatively analyze the tracking performance of the curved pipeline, we also analyzed the lateral position deviation and direction angle during the underwater pipeline tracking process. As shown in Fig. 16, the lateral position deviation of the underwater vehicle is within 3.0cm, and its average deviation is 1.2cm. On the other hand, the direction angle of the vehicle shows obvious stage variation. In the tracking stage of straight pipeline 1, the average direction angle is 4.5°. During the 45° turn tracking stage, the actual direction angle produced a deviation of 44° due to the abrupt change of the expected direction angle as the pipe turned, but the direction angle deviation is rapidly reduced under the action of the controller. In the tracking stage of straight pipeline 2, the average direction angle is 6.1°.

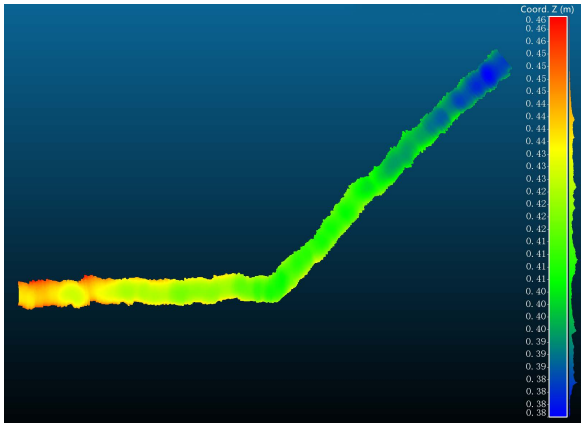

Fig. 17. 3D reconstruction result of underwater curved pipeline.

In addition, the 3D reconstruction result of the underwater curved pipeline is shown in Fig. 17. It can be seen that the basic shape of the acquired point cloud is consistent with the actual curved pipeline. We measured the diameter of the pipeline at different locations in the point cloud, and the average measurement error of the pipeline diameter was 4.5mm. At the same time, the turning angle of the pipeline in point cloud has been measured several times, and the average measurement error is 1.4°. The above experimental results demonstrate that the proposed underwater pipeline tracking and 3D reconstruction method can also achieve good performance for curved pipelines.

D. Spatial pipeline tracking and 3D reconstruction experiments

In order to further verify the effectiveness of the proposed method, we carried out underwater spatial pipeline tracking and 3D reconstruction experiments. The spatial pipeline is composed of pipeline 1 with a length of 0.6m and pipeline 2 with a length of 0.8m. One end of pipeline 2 is raised about 25cm in the vertical direction. The video acquisition sequence of underwater spatial pipeline tracking experiment is shown in Fig. 18.

In order to conduct quantitative analysis of the spatial pipeline tracking performance, the lateral position deviation and vertical position deviation during the pipeline tracking process were analyzed, which can be obtained with Eq. (6). As shown in Fig. 19, the lateral position deviation is within 2.5cm, and its average deviation is 1.1cm. Meanwhile, vertical position deviation is within 1.8cm, and its average deviation is 0.6cm.

In addition, the 3D reconstruction result of the underwater spatial pipeline is shown in Fig. 20. As can be seen that the basic shape of the acquired point cloud is consistent with the

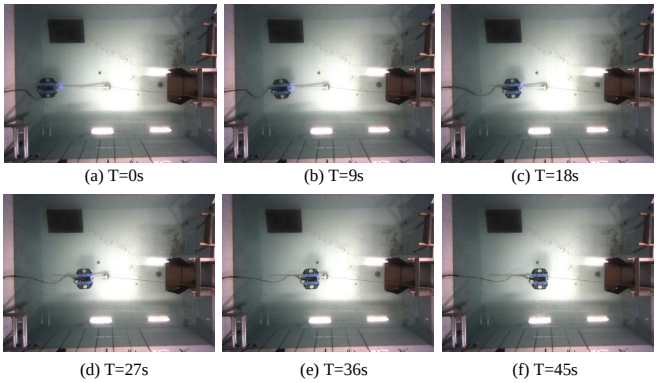

Fig. 18. Image sequences of the underwater spatial pipeline tracking.

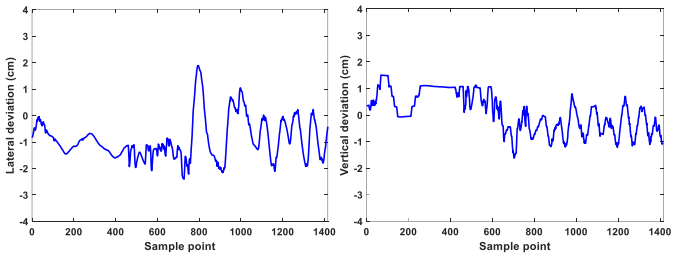

Fig. 19. Underwater spatial pipeline tracking. (a) Lateral position deviation. (b) Vertical deviation.

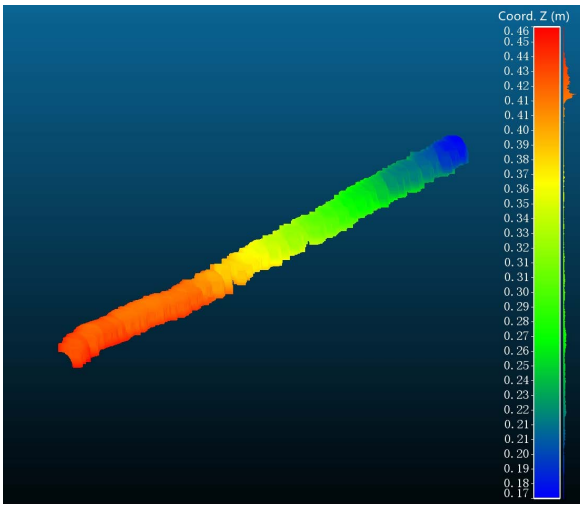

Fig. 20. 3D reconstruction result of underwater spatital pipeline.

TABLE IV
SPATIAL PIPELINE TRACKING AND 3D RECONSTRUCTION PERFORMANCE

Object	Lateral deviation	Vertical deviation	Diameter error
Spatial pipeline	2.5cm	1.8cm	5.6mm

actual spatial pipeline. By analyzing the point cloud, the end of pipeline 2 is approximately 25cm higher in the vertical direction than pipeline 1, which is also consistent with the actual spatial pipeline. At the same time, the diameter of the pipeline at different locations in the point cloud were measured and the average measurement error of the pipeline diameter was 5.6mm. Experimental results show that the proposed method could simultaneously realize the lateral and vertical direction tracking of underwater spatial pipeline, and obtain satisfactory tracking and 3D performance.

E. Discussion

The above experimental results show that the proposed SLV based pipeline tracking and 3D reconstruction method for underwater vehicle can achieve centimeter-level tracking accuracy and millimeter-level reconstruction accuracy. In order to prove the superiority of the proposed method, it is compared with the state-of-art underwater pipeline inspection methods. Due to the different measurement principle and experimental environment, it is difficult to make quantitative comparison. Therefore, qualitative comparison is adopted, and the comparison results are shown in Table V.

Currently, acoustic, magnetic, and optical methods are the main technical means for underwater pipeline inspection. Compared with acoustic based underwater pipeline inspection methods, the proposed method has higher pipeline positioning accuracy and 3D reconstruction accuracy, due to the shortcomings of acoustic methods such as low measurement accuracy and low resolution. Compared with magnetic based underwater pipeline inspection methods, the proposed method can achieve dense 3D reconstruction of pipelines, which is difficult to achieve for magnetic methods. Due to the severe absorption and scattering of light by water, passive light vision pipeline inspection methods have disadvantages such as sparse reconstructed point clouds and close measurement distances. Compared with passive light vision methods, the proposed method has advantages in reconstructing point cloud quality and measuring distance. In [26], [27], SLV based methods achieve dense 3D reconstruction of the interior of the pipeline. In fact, external inspection of pipelines is also very important, because some information of underwater pipelines can only be obtained through external inspection and underwater cable inspection can only be realized externally. Meanwhile, the external inspection of the pipeline is more challenging than the internal inspection, because underwater vehicle needs to track the pipeline. In this paper, the external inspection of the pipeline including underwater pipeline tracking and 3D reconstruction is realized.

In this paper, underwater pipeline tracking and 3D reconstruction experiments are carried out in a laboratory pool. Due to the relatively clear water quality and small water flow disturbance, all pipeline tracking experiments are successful. However, in future field experiments, the underwater environment will be complex including water turbidity and water flow interference. Therefore, in order to improve successful rate of underwater pipeline tracking, we will increase laser power to improve the measurement distance of SLV sensor firstly. Then, lightweight deep neural networks are combined to achieve accurate feature extraction of laser stripe images. Besides, more advanced control algorithms are adopted to realize underwater pipeline tracking control. Moreover, when conducting long-distance pipeline tracking and 3D reconstruction in the field, we will improve dead reckoning accuracy by integrating high-precision Fiber-optic inertial navigation system and DVL.

TABLE V
COMPARISON OF THE STATE-OF-ART UNDERWATER PIPELINE INSPECTION METHODS

Characteristics	[9-13]	[14-16]	[20-23]	[26-27]	**Our method**
Working principle	Acoustic	Magnetic	Passive vision	Structured light vision	**Structured light vision**
Positioning ability	Low accuracy	High accuracy	High accuracy	No	**High accuracy**
Reconstruction ability	Low accuracy	No	Medium accuracy	High accuracy	**High accuracy**
Measurement distance	Long	Medium	Short	Medium	**Medium**

VI. CONCLUSIONS

In this paper, an underwater pipeline tracking and 3D reconstruction method for underwater vehicle based on SLV is proposed. The system description, underwater pipeline positioning and tracking method, and underwater pipeline 3D reconstruction method are discussed in detail. Especially, some conclusions are summarized as follows:

1) A dual-line laser SLV sensor is developed, and a new underwater pipeline positioning method is proposed, which can simultaneously obtain the lateral deviation, height deviation and heading deviation under weak light water environment.
2) By combining laser stripe image feature points, refracted underwater SLV model and DVL information, the tracking and dense 3D reconstruction of underwater pipeline are realized simultaneously.
3) By integrating the self-designed underwater SLV sensor with the underwater vehicle BlueROV, an underwater pipeline tracking and 3D reconstruction system is developed and a series of planar and spatial pipeline experiments are conducted. Experiment results show that the lateral position deviation and vertical position deviation are less than 3.0cm and 2.0cm, and dense 3D point clouds of underwater pipeline can be acquired.

In the future, field experiments on underwater pipeline tracking and 3D reconstruction will be carried out.

REFERENCES

[1] S. Mukherjee, R. Zhang, M. Alzuhiri, V. V. Rao, L. Udpa, and Y. Deng, "Inline pipeline inspection using hybrid deep learning aided endoscopic laser profiling," *Journal of Nondestructive Evaluation*, vol. 41, no. 3, p. 56, 2022.

[2] Z. Chu, F. Wang, T. Lei, and C. Luo, "Path planning based on deep reinforcement learning for autonomous underwater vehicles under ocean current disturbance," *IEEE Transactions on Intelligent Vehicles*, vol. 8, no. 1, pp. 108–120, 2022.

[3] D. Ma, X. Chen, W. Ma, H. Zheng, and F. Qu, "Neural network model-based reinforcement learning control for auv 3-d path following," *IEEE Transactions on Intelligent Vehicles*, 2023.

[4] C. Lin, Y. Cheng, X. Wang, J. Yuan, and G. Wang, "Transformer-based dual-channel self-attention for uuv autonomous collision avoidance," *IEEE Transactions on Intelligent Vehicles*, 2023.

[5] X. Wang, C. Zhou, J. Wang, J. Fan, Z. Yin, C. Zhu, and L. Deng, "Cmbuv: A composite-mechanism bioinspired underwater vehicle integrated with elasticity and shear damping possesses high-performance capability," *IEEE Transactions on Intelligent Vehicles*, 2023.

[6] I. Jawhar, N. Mohamed, J. Al-Jaroodi, and S. Zhang, "An architecture for using autonomous underwater vehicles in wireless sensor networks for underwater pipeline monitoring," *IEEE Transactions on Industrial Informatics*, vol. 15, no. 3, pp. 1329–1340, 2018.

[7] R. Rayhana, Y. Jiao, Z. Bahrami, Z. Liu, A. Wu, and X. Kong, "Valve detection for autonomous water pipeline inspection platform," *IEEE/ASME Transactions on Mechatronics*, vol. 27, no. 2, pp. 1070–1080, 2021.

[8] X. Wang, J. Fan, S. Deng, Z. Wu, C. Zhou, Y. Ou, and Y. Han, "An underwater structured light vision calibration method considering unknown refractive index based on aquila optimizer," *IEEE Transactions on Instrumentation and Measurement*, vol. 72, pp. 1–12, 2022.

[9] T. O. Sæbø, H. J. Callow, P. E. Hagen, K. Maritime, and P. Espen, "Pipeline inspection with synthetic aperture sonar," in *Proceedings of the 33th Scandinavian Symposium on Physical Acoustics*, 2010.

[10] J. Carballini and F. Viana, "Using synthetic aperture sonar as an effective tool for pipeline inspection survey projects," in *2015 IEEE/OES Acoustics in Underwater Geosciences Symposium (RIO Acoustics)*. IEEE, 2015, pp. 1–5.

[11] A. Bagnitsky, A. Inzartsev, A. Pavin, S. Melman, and M. Morozov, "Side scan sonar using for underwater cables & pipelines tracking by means of auv," in *2011 IEEE Symposium on Underwater Technology and Workshop on Scientific Use of Submarine Cables and Related Technologies*. IEEE, 2011, pp. 1–10.

[12] V. Bharti, D. Lane, and S. Wang, "Robust subsea pipeline tracking with noisy multibeam echosounder," in *2018 IEEE/OES Autonomous Underwater Vehicle Workshop (AUV)*. IEEE, 2018, pp. 1–5.

[13] T. Kasetkasem, Y. Tipsuwan, S. Tulsook, A. Muangkasem, A. Leangaramkul, and P. Hoonsuwan, "A pipeline extraction algorithm for forward-looking sonar images using the self-organizing map," *IEEE Journal of Oceanic Engineering*, vol. 46, no. 1, pp. 206–220, 2020.

[14] X. Xiang, C. Yu, Z. Niu, and Q. Zhang, "Subsea cable tracking by autonomous underwater vehicle with magnetic sensing guidance," *Sensors*, vol. 16, no. 8, p. 1335, 2016.

[15] V. Bharti, D. Lane, and S. Wang, "A semi-heuristic approach for tracking buried subsea pipelines using fluxgate magnetometers," in *2020 IEEE 16th International Conference on Automation Science and Engineering (CASE)*. IEEE, 2020, pp. 469–475.

[16] C. Shili, W. Jialin, H. Xinjing, and L. Jian, "An accurate localization method for subsea pipelines by using external magnetic fields," *Measurement*, vol. 147, p. 106803, 2019.

[17] R. Rayhana, Y. Jiao, A. Zaji, and Z. Liu, "Automated vision systems for condition assessment of sewer and water pipelines," *IEEE Transactions on Automation Science and Engineering*, vol. 18, no. 4, pp. 1861–1878, 2020.

[18] J. Fan, X. Wang, C. Zhou, Y. Ou, F. Jing, and Z. Hou, "Development, calibration, and image processing of underwater structured light vision system: A survey," *IEEE Transactions on Instrumentation and Measurement*, vol. 72, pp. 1–18, 2023.

[19] J. Yan, K. You, W. Cao, X. Yang, and X. Guan, "Binocular vision-based motion planning of an auv: A deep reinforcement learning approach," *IEEE Transactions on Intelligent Vehicles*, 2023.

[20] R. Rayhana, H. Yun, Z. Liu, and X. Kong, "Automated defect-detection system for water pipelines based on cctv inspection videos of autonomous robotic platforms," *IEEE/ASME Transactions on Mechatronics*, 2023.

[21] M. Narimani, S. Nazem, and M. Loueipour, "Robotics vision-based system for an underwater pipeline and cable tracker," in *Oceans 2009-Europe*. IEEE, 2009, pp. 1–6.

[22] G. L. Foresti, "Visual inspection of sea bottom structures by an autonomous underwater vehicle," *IEEE Transactions on Systems, Man, and Cybernetics, Part B (Cybernetics)*, vol. 31, no. 5, pp. 691–705, 2001.

[23] G. Allibert, M.-D. Hua, S. Krupínski, and T. Hamel, "Pipeline following by visual servoing for autonomous underwater vehicles," *Control Engineering Practice*, vol. 82, pp. 151–160, 2019.

[24] Y. Ou, J. Fan, C. Zhou, S. Tian, L. Cheng, and M. Tan, "Binocular structured light 3-d reconstruction system for low-light underwater environments: Design, modeling, and laser-based calibration," *IEEE Transactions on Instrumentation and Measurement*, vol. 72, pp. 1–14, 2023.

[25] A. Inzartsev, G. Eliseenko, M. Panin, A. Pavin, V. Bobkov, and M. Morozov, "Underwater pipeline inspection method for auv based on laser line

recognition: Simulation results," in *2019 IEEE Underwater Technology (UT)*. IEEE, 2019, pp. 1–8.
[26] A. Gunatilake, L. Piyathilaka, A. Tran, V. K. Vishwanathan, K. Thiyagarajan, and S. Kodagoda, "Stereo vision combined with laser profiling for mapping of pipeline internal defects," *IEEE Sensors Journal*, vol. 21, no. 10, pp. 11 926–11 934, 2020.
[27] M. Montoya, Y. Montelongo, N. Jiang, S. M. Morris, and J. Parra-Michel, "Free-form laser profilometry for pipeline inspection and 3d cylindrical reconstructions," *IEEE Sensors Journal*, vol. 22, no. 1, pp. 297–303, 2021.
[28] Z. Wang, J. Fan, F. Jing, S. Deng, M. Zheng, and M. Tan, "An efficient calibration method of line structured light vision sensor in robotic eye-in-hand system," *IEEE Sensors Journal*, vol. 20, no. 11, pp. 6200–6208, 2020.
[29] J. Fan, X. Wang, C. Zhou, P. Zhang, F. Jing, and Z. Hou, "Structured light vision 3-d reconstruction system for different media considering refraction: Design, modeling, and calibration," *IEEE/ASME Transactions on Mechatronics*, 2023.
[30] A. Agrawal, S. Ramalingam, Y. Taguchi, and V. Chari, "A theory of multi-layer flat refractive geometry," in *2012 IEEE conference on computer vision and pattern recognition*. IEEE, 2012, pp. 3346–3353.
[31] A. Bodenmann, B. Thornton, and T. Ura, "Generation of high-resolution three-dimensional reconstructions of the seafloor in color using a single camera and structured light," *Journal of Field Robotics*, vol. 34, no. 5, pp. 833–851, 2017.

Junfeng Fan received the B.S. degree in mechanical engineering and automation from Beijing Institute of Technology, Beijing, China, in 2014 and Ph.D. degree in control theory and control engineering from the Institute of Automation, Chinese Academy of Sciences (IACAS), Beijing, China, in 2019.

He is currently an Associate Professor of Control Theory and Control Engineering with the State Key Laboratory of Management and Control for Complex Systems, IACAS, Beijing. His research interests include robot vision and underwater robot.

Yaming Ou Yaming Ou received the B.E. degree in automation from Southeast University, Nanjing, China in 2021. He is currently pursuing the Ph.D. degree in control theory and control engineering with the Institute of Automation, Chinese Academy of Sciences (IACAS), Beijing, China. His research interests include perception and intelligent control of underwater robots.

Xuan Li received his Ph.D. degree in Control Science and Engineering from the Beijing Institute of Technology, Beijing, China, in 2020. From October 2018 to October 2019, he was a Visiting Scholar at the Department of Computer Science, Stony Brook University, Stony Brook, NY, USA. After that, he joined the Peng Cheng Laboratory and became a Postdoctoral Research Associate at the Virtual Reality Laboratory.

He is currently an Associate Research Professor at Peng Cheng Laboratory. His research interests include intelligent vehicles, scene reconstruction, image synthesis, collaborative perception or control, bionic vision computing.

Chao Zhou received the B.S. degree in automation from Southeast University, Nanjing, China, in 2003 and the Ph.D. degree in control theory and control engineering from the Institute of Automation, Chinese Academy of Sciences (IACAS), Beijing, China, in 2008.

He is currently a Professor of the Laboratory of Cognition and Decision Intelligence for Complex Systems at IACAS, Beijing. His research interests include underwater robot and bionic robot.

Zengguang Hou received the B.E. and M.E. degrees in electrical engineering from Yanshan University (formerly North-East Heavy Machinery Institute), Qinhuangdao, China, in 1991 and 1993, respectively, and the Ph.D. degree in electrical engineering from the Beijing Institute of Technology, Beijing, China, in 1997.

From May 1997 to June 1999, he was a PostDoctoral Research Fellow with the Key Laboratory of Systems and Control, Institute of Systems Science, Chinese Academy of Sciences, Beijing. He was a Research Assistant with The Hong Kong Polytechnic University, Hong Kong, from May 2000 to January 2001. From July 1999 to May 2004, he was an Associate Professor with the Institute of Automation, Chinese Academy of Sciences, where he has been a Full Professor since June 2004. From September 2003 to October 2004, he was a Visiting Professor with the Intelligent Systems Research Laboratory, College of Engineering, University of Saskatchewan, Saskatoon, SK, Canada. He is currently a Professor with the State Key Laboratory of Multimodal Artificial Intelligence Systems, IACAS, Beijing. His research interests include neural networks, robotics, and intelligent systems.

View publication stats